

See discussions, stats, and author profiles for this publication at: <https://www.researchgate.net/publication/231274618>

# Selective Production of Aromatics by Crude Bio-oil Valorization with a Nickel-Modified HZSM-5 Zeolite Catalyst

ARTICLE in ENERGY & FUELS · JANUARY 2010

Impact Factor: 2.79 · DOI: 10.1021/ef901231j

CITATIONS

72

READS

73

## 5 AUTHORS, INCLUDING:



**Beatriz Valle**

Universidad del País Vasco / Euskal Herriko ...

31 PUBLICATIONS 801 CITATIONS

SEE PROFILE



**Ana G. Gayubo**

Universidad del País Vasco / Euskal Herriko ...

129 PUBLICATIONS 3,097 CITATIONS

SEE PROFILE



**Andrés T. Aguayo**

Universidad del País Vasco / Euskal Herriko ...

155 PUBLICATIONS 3,839 CITATIONS

SEE PROFILE



**Martin Olazar**

Universidad del País Vasco / Euskal Herriko ...

274 PUBLICATIONS 5,689 CITATIONS

SEE PROFILE

## Selective Production of Aromatics by Crude Bio-oil Valorization with a Nickel-Modified HZSM-5 Zeolite Catalyst

Beatriz Valle,\* Ana G. Gayubo, Andrés T. Aguayo, Martin Olazar, and Javier Bilbao

Chemical Engineering Department, University of the Basque Country, P.O. Box 644, 48080, Bilbao, Spain

Received October 28, 2009. Revised Manuscript Received January 8, 2010

The transformation of crude bio-oil to hydrocarbons has been studied in an online thermal catalytic process that is comprised of two steps: the thermal treatment reactor, followed by the catalytic reactor. The deposition of pyrolytic lignin formed by the polymerization of biomass-derived products is enhanced in the thermal step. Volatiles are processed in a fluidized-bed reactor with a catalyst that is hydrothermally stable and selective for aromatic production, which is based on a HZSM-5 zeolite modified by the incorporation of 1 wt % of nickel. The effect of operating conditions (temperature, space time, and time-on-stream), as well as feedstock ratio, on bio-oil conversion, product lump yields, and the selectivity of aromatics has been studied. These conditions also have a significant effect on deactivation, which is attributed to coke deposit on the catalyst. The temperature-programmed oxidation (TPO) curves of coke combustion allow the identification of two fractions: one of thermal origin (pyrolytic lignin) and the other of catalytic origin, whose formation is dependent on the concentration of oxygenates in the reaction medium. A feed with 60 wt % methanol, at 450 °C, with a space time of 0.371 (g of catalyst) h (g of oxygenates)<sup>−1</sup> allows one to obtain 90 wt % conversion of the bio-oil in the feed in the catalytic transformation step, with a selectivity of aromatics of 0.4 (benzene, toluene, xylenes (BTX) selectivity of 0.25). These results remain almost constant in the first hour of reaction. The yields of CO and CO<sub>2</sub> are low, because their formation is attenuated by co-feeding methanol.

### 1. Introduction

To cope with the increasing energy consumption in a scenario of fossil fuel depletion and climate change due to greenhouse gases, alternative renewable sources are now being investigated by many institutions across the world. Biomass and its derivatives have been identified as an alternative feedstock for partially replacing petroleum as a raw material for obtaining fuels, hydrocarbons for petrochemical synthesis, and hydrogen.<sup>1,2</sup> A route of growing interest is the flash pyrolysis of lignocellulosic biomass and the subsequent incorporation of the liquid product (bio-oil) as feed in a refinery.<sup>3–5</sup> The main advantage of this route is that the entire process is divided into two stages. The first step, flash pyrolysis, may be performed by processing the geographically dispersed biomass sources with small-scale units. The second step involves the incorporation of bio-oil as additional feed to the refinery, together with other streams, either from the refinery itself or from other alternative raw materials. This strategy would allow operation at a large scale by treating the intermediate and final products together with petroleum derivatives, using the same reaction and separation units.<sup>6</sup> However, the industrial implementation of these initiatives requires laboratory experimentation and existing information is still limited. The co-feed in fluid catalytic cracking (FCC)

units of biomass derivatives, such as glycerol and sorbitol, along with vacuum gas oil,<sup>7</sup> or hydrodeoxygenation of guaya-col or the latter, together with straight-run gas oil,<sup>8,9</sup> provides encouraging results, maintaining the quality of products.

Nevertheless, feeding crude bio-oil into refinery units has serious difficulties, because of the complex composition of crude bio-oil (depending on the biomass), its instability, and the deposition of carbonaceous material (denoted as pyrolytic lignin) in the volatilization step by polymerization of mainly phenolic components derived from the pyrolysis of lignocellulosic biomass lignin.<sup>10</sup>

Bio-oil is a polar and hydrophilic brown liquid, which is composed of products from the depolymerization and fragmentation of cellulose, hemicellulose, and lignin, with a water content of ~25 wt %, and an oxygen content of 45–50 wt %. Over 300 components have been identified using gas chromatography-mass spectroscopy (GC-MS) (such as acids, alcohols, aldehydes, esters, ketones, phenols, guaiacols, syringols, sugars, furans, alkenes, aromatics, nitrogen compounds, and a variety of oxygen compounds). These components may be grouped into five families: (1) hydroxyacetaldehydes, (2) hydroxyketones, (3) sugars, (4) carboxylic acids, and (5) phenolic compounds.<sup>11,12</sup> Because of the complex nature of

\*Author to whom all correspondence should be addressed. Phone: +34 946 015361. Fax: +34 946 013 500. E-mail: beatriz.valle@ehu.es.

(1) Huber, G. W.; Iborra, S.; Corma, A. *Chem. Rev.* **2006**, *106*, 4044–4098.

(2) Corma, A.; Iborra, S.; Velty, A. *Acc. Chem. Rev.* **2007**, *107*, 2411–2502.

(3) Czernik, S.; Bridgwater, A. V. *Energy Fuels* **2004**, *18*, 590–598.

(4) Mohan, D.; Pittman, C. U.; Steele, P. H. *Energy Fuels* **2006**, *20*, 848–889.

(5) Stöcker, M. *Angew. Chem., Int. Ed.* **2008**, *48*, 9200–9211.

(6) Huber, G. W.; Corma, A. *Angew. Chem., Int. Ed.* **2007**, *46*, 7184–7201.

(7) Corma, A.; Huber, G. W.; Sauvanaud, L.; O'Connor, P. *J. Catal.* **2007**, *247*, 307–327.

(8) Gutierrez, A.; Kaila, R. K.; Honkela, M. L.; Slioor, R.; Krause, A. O. I. *Catal. Today* **2008**, *147*, 239–246.

(9) Bui, V. N.; Toussaint, G.; Laurenti, D.; Mirodatos, C.; Geantet, C. *Catal. Today* **2009**, *143*, 172–178.

(10) Samolada, M. C.; Baldauf, W.; Vasalos, I. A. *Fuel* **1998**, *77*, 1667–1675.

(11) Aguado, R.; Olazar, M.; San José, M. J.; Aguirre, G.; Bilbao, J. *Ind. Eng. Chem. Res.* **2000**, *39*, 1925–1933.

(12) Branca, C.; Giudicianni, P.; Di Blasi, C. *Ind. Eng. Chem. Res.* **2003**, *42*, 3190–3202.

bio-oil, and because of its instability, the bio-oil can undergo repolymerization during storage, which would result in an increase in viscosity and molecular weight. This could lead to an increase in higher-molecular-weight compounds such as levoglucosan, and a decrease in the bio-oil volatility and in lower-molecular-weight compounds such as hydroxyacetaldehyde.<sup>13</sup> The addition of 10 wt % methanol achieves crude bio-oil stabilization during its storage.<sup>14</sup>

The repolymerization of bio-oil components (and, particularly, of pyrolysis lignin derivatives) is a barrier for the valorization of crude bio-oil by catalytic transformation as the deposition of pyrolytic lignin (with a yield of ~20 wt %) causes the rapid deactivation of the catalyst and even gas flow blockage. Consequently, much of the experimental study of catalytic transformation was limited to the pure compounds that comprise the bio-oil, which has been the basis for catalysts discrimination and the study of reaction mechanisms and conditions, in two catalytic transformation routes: (i) reforming for obtaining  $H_2$ <sup>15,16</sup> and (ii) dehydration–cracking to obtain hydrocarbons.<sup>17,18</sup>

For a water content in the bio-oil of > 50 wt %, the liquid is separated into two phases: aqueous and organic. Studies have also been conducted on the catalytic transformation of the aqueous fraction of bio-oil, which also involves serious problems of pyrolytic lignin deposition, although to a lesser extent than crude bio-oil volatilization.<sup>19,20</sup>

The transformation of the entire “crude” bio-oil is a goal for maximizing the valorization of all the carbon and hydrogen contained in the lignocellulosic biomass, and there are several initiatives in this field. Lappas et al.<sup>21</sup> have studied crude bio-oil hydrotreatment and subsequent co-feeding with vacuum gas oil into catalytic cracking units (FCC). Gayubo et al.<sup>22,23</sup> have found that methanol co-feeding attenuates pyrolytic lignin deposition and that this strategy is effective in an online two-step process (thermal–catalytic) in which the pyrolytic lignin is separated in the first step, where its controlled deposition occurs. The remaining volatiles are processed online in a fluidized-bed reactor in which the deposition of a small amount of remaining pyrolytic lignin has a smaller impact on deactivation than acid site blockage by catalytic coke.

This combined strategy (co-feeding of methanol and pyrolytic lignin separation) is applied in this paper (see Figure 1) and a study is conducted on the effect of the operating conditions on product distribution in the catalytic step of the two-step process, with the aim of obtaining a high selectivity of BTX aromatics. Furthermore, special attention

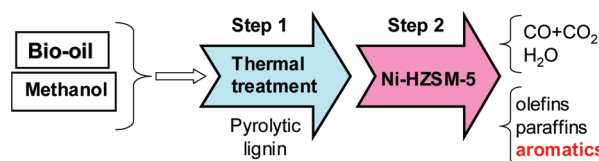


**Figure 1.** Two-step process (thermal treatment–catalytic transformation) for the transformation of bio-oil/methanol mixtures into hydrocarbons.

**Table 1. Component Families in the Crude Bio-oil**

component	wt %
acetic acid	15.3
acetone	5.3
other ketones	21.8
other acids and esters	10.8
hydroxyacetaldehyde	10.6
other aldehydes	8.7
phenols	8.2
alcohols	11.6
ethers	0.9
levoglucosan	3.9
others	1.3
non-identified	1.6

has been given to the objectives of reducing catalyst deactivation and CO and CO<sub>2</sub> yields. The incorporation of a transition metal (nickel) in the HZSM-5 zeolite is considered to increase the yield of aromatics<sup>24</sup> and the hydrothermal stability of the catalyst.<sup>25</sup> This behavior is attributable to the dehydrogenating activity of nickel and to the fact that the doped catalyst has moderate acid strength.

## 2. Experimental Section

**2.1. Bio-oil Production and Composition.** The bio-oil has been obtained at 450 °C using a N<sub>2</sub> stream in a pilot plant provided with a conical spouted-bed reactor.<sup>11,26</sup> The feedstock used to produce bio-oil was pine (*Pinus insignis*) sawdust with a particle size between 0.8 mm and 2 mm. The bio-oil used in this study corresponds to a 75–76 wt % fraction of the entire bio-oil, given that, to attain product reproducibility, the bio-oil studied is that collected in the condenser and in the ice–water trap, whereas that retained in the coalescence filter has been discarded. The composition of the crude bio-oil (see Table 1) was determined by GC/MS analysis in a GC/MS device (Shimadzu QP2010S) that was provided with a TBR-1MS column. Product identification was accomplished using the NIST 147 library. The quantitative analysis of the bio-oil components was based on peak area evaluation, and the correction factors for the chromatographic analysis were determined using 18 pattern mixtures containing the main components. In a previous paper, the detailed composition of individual components in the bio-oil is shown.<sup>23</sup> The elemental composition was CH<sub>1.84</sub>O<sub>0.59</sub>, and the average molecular weight was 100.2 g mol<sup>−1</sup>. The water content (48 wt % in the crude bio-oil) was measured via gas chromatography (Agilent Micro GC 3000).

**2.2. Reaction Equipment and Product Analysis.** The reaction equipment is shown in Figure 2. The thermal and catalytic cracking of the bio-oil is performed online in two separate units. In the first unit (a cylindrical tube made of S-316 stainless steel, with an internal diameter of 5/8 in.), the bio-oil is cooled with water at the inlet to avoid the condensation of pyrolytic lignin that is deposited on a bed of glass spheres at 400 °C. The second

(13) Fahmi, R.; Bridgwater, A. W.; Donnison, I.; Yates, N.; Jones, J. M. *Fuel* **2008**, *87*, 1230–1240.

(14) Diebold, J. P.; Czernik, S. *Energy Fuels* **1997**, *11*, 1081–1091.

(15) Bimbela, F.; Oliva, M.; Ruiz, J.; García, L.; Arauzo, J. *J. Anal. Appl. Pyrolysis* **2007**, *79*, 112–120.

(16) Ramos, M. C.; Navascués, A. I.; García, L.; Bilbao, R. *Ind. Eng. Chem. Res.* **2007**, *46*, 2399–2406.

(17) Gayubo, A. G.; Aguayo, A. T.; Atutxa, A.; Aguado, R.; Bilbao, J. *Ind. Eng. Chem. Res.* **2004**, *43*, 2610–2618.

(18) Gayubo, A. G.; Aguayo, A. T.; Atutxa, A.; Aguado, R.; Olazar, M. *Ind. Eng. Chem. Res.* **2004**, *43*, 2619–2626.

(19) Gayubo, A. G.; Aguayo, A. T.; Atutxa, A.; Prieto, R.; Bilbao, J. *Energy Fuels* **2004**, *18*, 1640–1647.

(20) Basagiannis, A. C.; Verykios, X. E. *Catal. Today* **2007**, *127*, 256–264.

(21) Lappas, A. A.; Bezergianni, S.; Vasalos, I. A. *Catal. Today* **2008**, *145*, 55–62.

(22) Gayubo, A. G.; Valle, B.; Aguayo, A. T.; Olazar, M.; Bilbao, J. *Energy Fuels* **2009**, *23*, 4129–4136.

(23) Gayubo, A. G.; Valle, B.; Aguayo, A. T.; Olazar, M.; Bilbao, J. *J. Chem. Technol. Biotechnol.* **2010**, *85*, 132–144.

(24) French, R.; Czernik, S. *Fuel Process. Technol.* **2010**, *91*, 25–32.

(25) Valle, B.; Alonso, A.; Atutxa, A.; Gayubo, A. G.; Bilbao, J. *Catal. Today* **2005**, *106*, 118–122.

(26) Olazar, M.; Aguado, R.; San José, M. J.; Bilbao, J. *J. Chem. Technol. Biotechnol.* **2001**, *76*, 469–476.

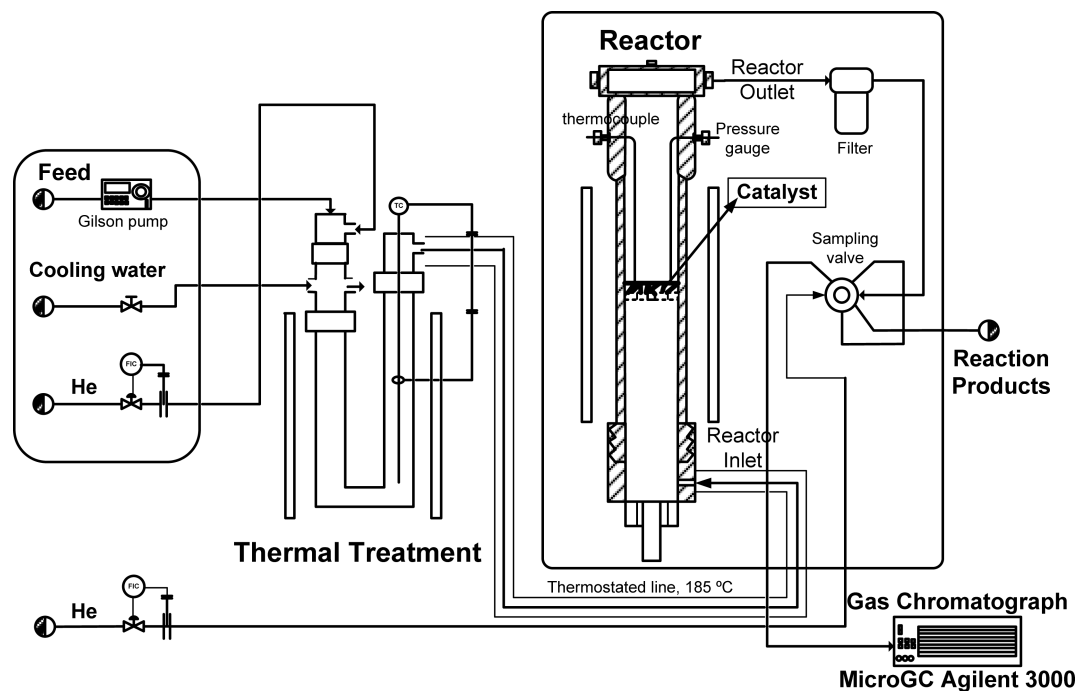


Figure 2. Schematic of the reaction equipment.

unit performs a catalytic transformation of the volatile compounds that are leaving the first unit. It is a fluidized-bed reactor (inside a vertical cylindrical tube made of S-316 stainless steel, with an internal diameter of 20 mm and a total length of 465 mm) located within a ceramic chamber that is heated by an electrical resistance. The catalyst bed is placed on a porous plate (at a distance of 285 mm from the reactor base). The fluidized-bed reactor has advantages over the fixed bed in the transformation of oxygenates into hydrocarbons to attenuate deactivation.<sup>27</sup>

The online analysis of the products was performed every 5 min, with the samples being sent to a gas chromatograph (Agilent Micro GC 3000) that was provided with four modules, for the analysis of (1) permanent gases ( $O_2$ ,  $N_2$ ,  $H_2$ ,  $CO$ ,  $CH_4$ ); (2) oxygenates (MeOH, dimethyl ether,  $CO_2$ ), light olefins ( $C_2$ – $C_3$ ) and water; (3)  $C_2$ – $C_6$  hydrocarbons; and (4)  $C_6$ – $C_{12}$  hydrocarbons and oxygenate compounds. The volatile compounds that do not reach the analysis equipment are cooled in a Peltier condenser ( $0\text{ }^\circ\text{C}$ ), from which two streams leave: (1) incondensable compounds that leave the reaction equipment through the outlet for gases and (2) the liquid fraction that is collected in a vessel placed on a digital balance (Electronic Balances EK-600H). Data gathering and processing are performed using the software Soprane (Version 2.4.b).

**2.3. Catalyst.** The catalyst (Ni-Z-30) is prepared from HZSM-5 zeolite (with a  $SiO_2/Al_2O_3$  ratio of 30) modified by the incorporation of 1 wt % of nickel. This composition is suitable for striking a good balance between activity and hydrothermal stability, as has been proven in the transformation of aqueous methanol (50 wt % water) at high temperature.<sup>25</sup> The commercial zeolite (Zeolyst Int.) is supplied in ammonium form, and, to obtain the acid form, it has been calcined following a temperature sequence (up to  $570\text{ }^\circ\text{C}$ ). Impregnation with nickel has been accomplished by slowly adding a  $Ni(NO_3)_2$  dissolution into the acid form zeolite under vacuum (in a Rotavapor) at  $80\text{ }^\circ\text{C}$ . The active phase is dried for 24 h at  $110\text{ }^\circ\text{C}$  and subsequently agglomerated (by wet extrusion) with bentonite (Exaloid) and using alumina (Prolabo) that had been calcined at  $1000\text{ }^\circ\text{C}$  as an

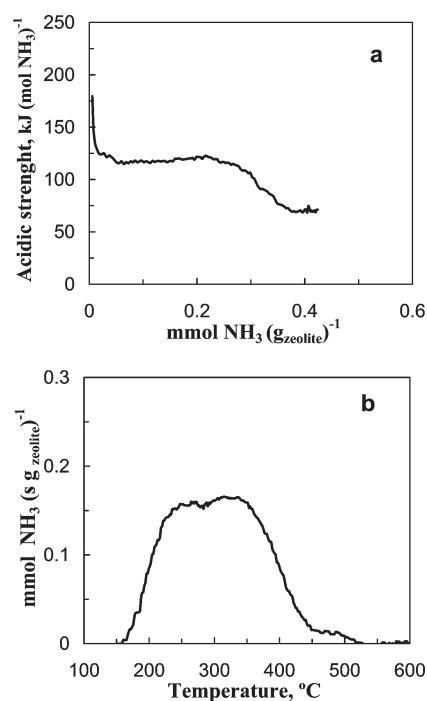


Figure 3. Catalyst acidity: (a) acid strength distribution and (b) temperature-programmed desorption (TPD) of  $NH_3$  adsorbed at  $150\text{ }^\circ\text{C}$ .

inert charge. The proportion of each component in the catalyst is 25 wt % zeolite, 45 wt % bentonite, and 30 wt % alumina. The extrudates are dried at room temperature for 24 h. Subsequently, the particles are ground and sieved to a size between 0.15 mm and 0.25 mm, dried at  $110\text{ }^\circ\text{C}$  for 24 h, and calcined at  $575\text{ }^\circ\text{C}$  for 2 h. This temperature is reached following a heating rate of  $5\text{ }^\circ\text{C min}^{-1}$ .

The physical properties ( $S_{BET} = 178\text{ m}^2\text{ g}^{-1}$ ;  $V_p = 0.57\text{ cm}^3\text{ g}^{-1}$ , and pore volume distribution,  $d_p < 20\text{ }\text{\AA}$ , 4.2%;  $20\text{ }\text{\AA} < d_p < 500\text{ }\text{\AA}$ , 37.8%; and  $d_p > 500\text{ }\text{\AA}$ , 58.0%) have been determined by  $N_2$  adsorption–desorption (Micromeritics ASAP 2010)

(27) Aguayo, A. T.; Gayubo, A. G.; Ortega, J. M.; Olazar, M.; Bilbao, J. *Catal. Today* **1997**, 37, 239–248.



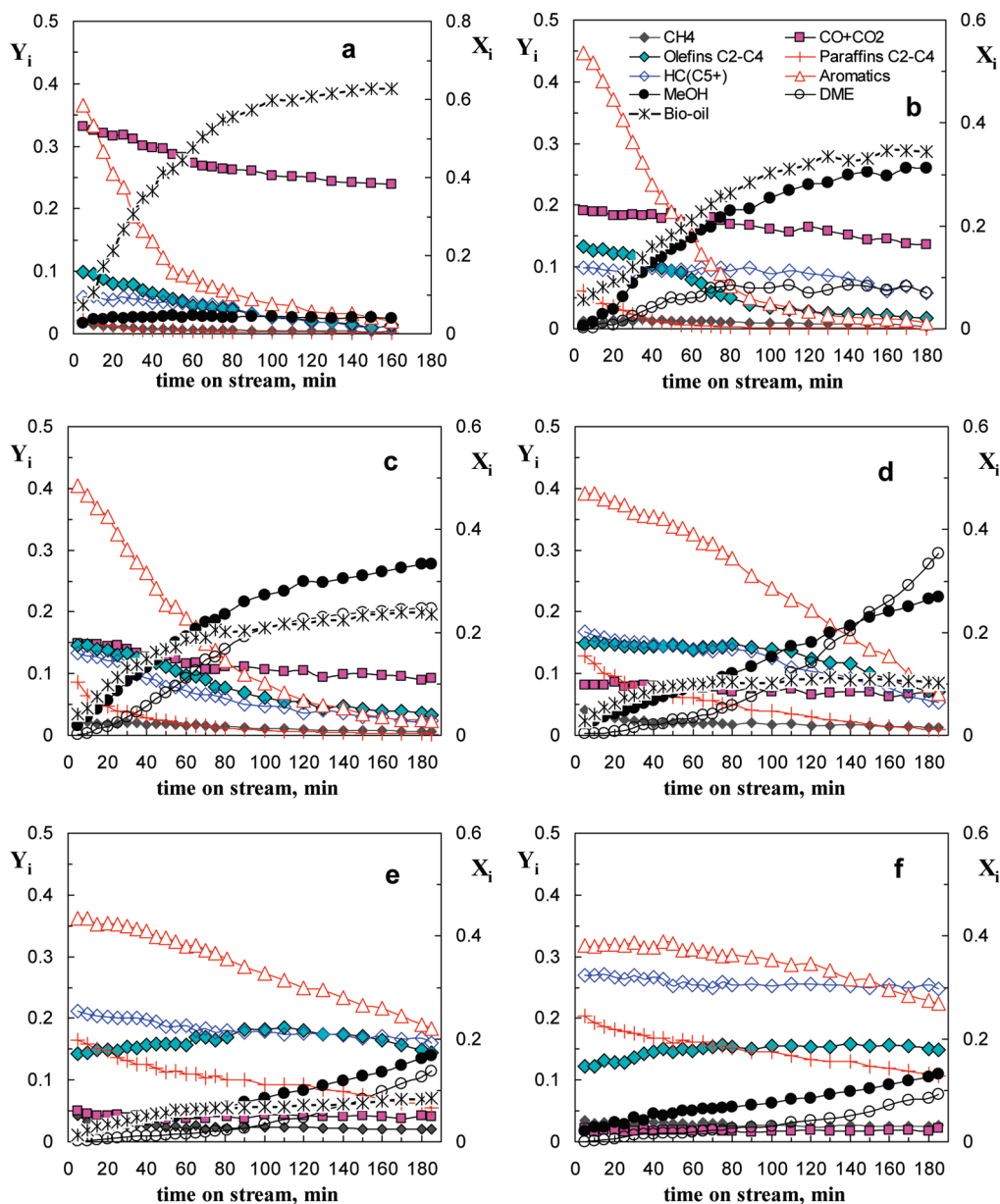


**Figure 4.** Effect of methanol content in the feed on the evolution with the time-on-stream of product lump yields ( $Y_i$ , left axis) and oxygenate mass fraction ( $X_i$ , right axis) in the reactor outlet stream: (a) feed, crude bio-oil; (b) feed with 20 wt % methanol; (c) feed with 40 wt % methanol; (d) feed with 60 wt % methanol; (e) feed with 80 wt % methanol; and (f) feed, pure methanol. Reaction conditions: 450 °C;  $W/F_0 = 0.371$  (g of catalyst) h (g of oxygenates) $^{-1}$ .

and mercury porosimetry (Micromeritics Autopore 9220). The total acidity (0.41 (mmol of  $\text{NH}_3$ ) (g of zeolite) $^{-1}$ ) and acid strength distribution have been determined by measuring the differential adsorption of  $\text{NH}_3$  at 150 °C (see Figure 3a) and the subsequent temperature-programmed desorption (TPD) of the adsorbed  $\text{NH}_3$  by following a temperature ramp of 5 °C  $\text{min}^{-1}$  up to 550 °C (see Figure 3b).<sup>28,29</sup> The equipment used was a thermobalance (TA Instruments SDT 2960) that was online with a mass spectrometer (Thermostar, Balzers Instruments). The Brönsted/Lewis acid sites ratio has been determined by Fourier transform infrared (FTIR) analysis (Nicolet 6700 equipped with a Specac catalytic chamber), from the ratio between the intensity of the adsorption bands at 1545 and 1450  $\text{cm}^{-1}$  of pyridine adsorbed at 150, 250, and

350 °C, and the results of this ratio are 0.49, 0.56 and 0.61, respectively.

The coke deposited on the catalyst has been studied by combustion with air in the TG/MS arrangement previously described. Subsequent to a coke aging step in a helium stream at 550 °C for 1 h (to attain reproducible results), combustion is accomplished using 25%  $\text{O}_2$  in helium, following a ramp of 3 °C  $\text{min}^{-1}$  from 300 °C to 550 °C, and maintaining this temperature for 1 h.<sup>30</sup> Throughout combustion, the following data are monitored: temperature, mass, temperature difference between sample and reference, and the intensity in the mass spectrometer for the signals corresponding to the masses 18 (water), 28 (CO), and 44 ( $\text{CO}_2$ ). Combustion is complete when all the carbon in the coke is volatilized as  $\text{CO}_2$ . Signals corresponding to the presence of other compounds, such as  $\text{SO}_2$  or  $\text{NO}_x$ , were insignificant.

(28) Aguayo, A. T.; Gayubo, A. G.; Ereña, J.; Olazar, M.; Arandes, J. M.; Bilbao, J. J. *Chem. Technol. Biotechnol.* **1994**, *60*, 141–146.

(29) Gayubo, A. G.; Benito, P. L.; Aguayo, A. T.; Olazar, M.; Bilbao, J. J. *Chem. Technol. Biotechnol.* **1996**, *65*, 186–192.

(30) Ortega, J.; Gayubo, A. G.; Aguayo, A. T.; Benito, P. L.; Bilbao, J. *Ind. Eng. Chem. Res.* **1997**, *36*, 60–66.

### 3. Results

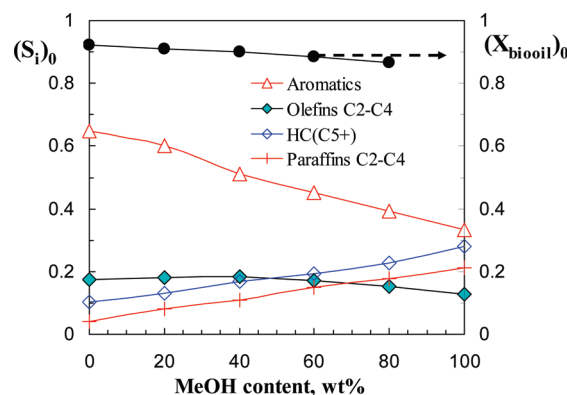
**3.1. Effect of Methanol Co-feeding.** Methanol is known to be effective in stabilizing crude bio-oil for its storage.<sup>14</sup> Furthermore, methanol co-feeding reduces the yield of pyrolytic lignin in the bio-oil thermal treatment step (first unit in Figure 2).<sup>22</sup> The results described below show that methanol co-feeding also provides advantages in the subsequent catalytic transformation step (second unit in Figure 2).

Figure 4 shows the results of the evolution with the time-on-stream of product yields ( $Y_i$ , left axis) and mass fraction, on a water-free basis, of oxygenates (methanol, dimethyl ether, and bio-oil components) at the reactor outlet ( $X_i$ , right axis). The results correspond to a temperature of 450 °C and a space time of 0.371 (g of catalyst) h (g of oxygenates)<sup>−1</sup> and each graph corresponds to a feed with different methanol content. The products are grouped into the following compounds: CH<sub>4</sub>, CO + CO<sub>2</sub>, aromatics, C<sub>2</sub>–C<sub>4</sub> olefins, C<sub>2</sub>–C<sub>4</sub> paraffins, and nonaromatic C<sub>5+</sub> compounds. Dimethyl ether (DME) is almost in thermodynamic equilibrium with methanol from the reactor entrance, so it has been considered to be a reactant. Product yields ( $Y_i$ ) were calculated from the chromatographic results of each lump  $i$  at the fluidized-bed reactor outlet, expressed in terms of mass units of oxygenates in the feed:

$$Y_i = \frac{\text{mass flow rate of lump } i \text{ at the reactor outlet}}{\text{mass flow rate of oxygenates fed into the reactor}} \quad (1)$$

The formation of CO and CO<sub>2</sub> (by decarbonylation and decarboxylation of bio-oil oxygenates) is one of the main drawbacks facing the biomass valorization process by dehydration–cracking using acid catalysts, either in situ in a pyrolysis reactor<sup>31–34</sup> or in a reactor for reforming the volatiles produced in the pyrolysis.<sup>35,36</sup> Particularly, CO<sub>2</sub> formation contributes to the greenhouse effect, apart from decreasing the yield in the transformation of carbon to hydrocarbons.

The results in Figure 4a, corresponding to a feed of crude bio-oil, show that aromatics and CO + CO<sub>2</sub> lumps are the main products at zero time-on-stream. However, by increasing the methanol content in the feed, the yield of CO + CO<sub>2</sub> decreases at a greater rate than that corresponding to the content of bio-oil in the feed, which is evidence of a synergistic effect of methanol by promoting the competition of reactions for hydrocarbons formation over the reactions of decarbonylation and decarboxylation of bio-oil components. A very pronounced deactivation is also noteworthy (Figure 4a), whereby the aromatics yield decreases by about one-half within 30 min, although the decrease in light olefin yield, and especially in C<sub>5+</sub> hydrocarbons, is significantly lower. The yield of CO + CO<sub>2</sub> decreases much more slowly



**Figure 5.** Effect of methanol content in the feed on the evolution of bio-oil conversion (right axis) and on product lump selectivity (excluding CO and CO<sub>2</sub>) at zero time-on-stream (left axis) in the catalytic transformation step. Reaction conditions: 450 °C;  $W/F_0 = 0.371$  (g of catalyst) h (g of oxygenates)<sup>−1</sup>.

than that of hydrocarbon lumps and it is almost constant after 2 h, because of the thermal origin of the reactions that lead to these products. Catalyst deactivation attenuates by increasing the methanol content in the feed, which is especially significant for a methanol content of 60 wt %.

Figure 5 shows the effect of methanol content on bio-oil conversion, which has been calculated from the bio-oil mass flow rates at the fluidized-bed reactor inlet and outlet (denoted as  $(m_{\text{bio-oil}})_i$  and  $(m_{\text{bio-oil}})_o$ , respectively):

$$(X_{\text{bio-oil}})_{t=0} = \left[ \frac{(m_{\text{bio-oil}})_i - (m_{\text{bio-oil}})_o}{(m_{\text{bio-oil}})_i} \right]_{t=0} \quad (2)$$

As observed in Figure 5, bio-oil conversion at zero time-on-stream is high and decreases slightly by increasing the methanol content in the feed. This result must be attributed to the attenuating effect of the water formed in methanol dehydration on the bio-oil oxygenates transformation mechanisms. This hypothesis can be supported in the well-known effect of water for the conversion of oxygenates (methanol, ethanol) to hydrocarbons on HZSM-5 zeolite, SAPO-34, and SAPO-18 catalysts.<sup>37–39</sup> It is important to state that this effect is attributed to the competence of water with hydrocarbons in their adsorption on the acid sites and that this competence is efficient when water is formed in the dehydration of the oxygenate. This result is explained because, according to the mechanism, the water formed is adsorbed on the acid sites (given way to the hydration of Brönsted sites), whereas the adsorption of the water fed with bio-oil is of low significance, under the reaction conditions.

Figure 5 also shows the effect of methanol content on the selectivity of product lumps at zero time-on-stream, which has been calculated by mass unit of hydrocarbon products (without considering the yield of CO and CO<sub>2</sub>):

$$(S_i)_{t=0} = \left[ \frac{Y_i}{\sum_{\text{HC}} Y_i} \right]_{t=0} \quad (3)$$

(31) Lappas, A. A.; Samolada, M. C.; Iatridis, D. K.; Voutetakis, S.; Vasalos, I. A. *Fuel* **2002**, *81*, 2087–2095.

(32) Atutxa, A.; Aguado, R.; Gayubo, A. G.; Olazar, M.; Bilbao, J. *Energy Fuels* **2005**, *19*, 765–774.

(33) Adam, J.; Antonakou, E.; Lappas, A. A.; Stöcker, M.; Nilsen, M. H.; Bouzga, A.; Hustad, J. E.; Oye, G. *Microporous Mesoporous Mater.* **2006**, *96*, 93–101.

(34) Nilsen, M. H.; Antonakou, E.; Bouzga, A.; Lappas, A. A.; Maticen, K.; Stöcker, M. *Microporous Mesoporous Mater.* **2007**, *105*, 189–203.

(35) Horne, P. A.; Williams, P. T. *Fuel* **1995**, *75*, 1043–1050.

(36) Pütün, E.; Uzun, B. B.; Pütün, A. E. *Energy Fuels* **2009**, *23*, 2248–2258.

(37) Benito, P. L.; Gayubo, A. G.; Aguayo, A. T.; Castilla, M.; Bilbao, J. *Ind. Eng. Chem. Res.* **1996**, *35*, 81–89.

(38) Gayubo, A. G.; Aguayo, A. T.; Sánchez del Campo, A. E.; Tarrío, A. M.; Bilbao, J. *Ind. Eng. Chem. Res.* **2000**, *39*, 292–300.

(39) Gayubo, A. G.; Aguayo, A. T.; Alonso, A.; Bilbao, J. *Ind. Eng. Chem. Res.* **2007**, *46*, 1981–1989.

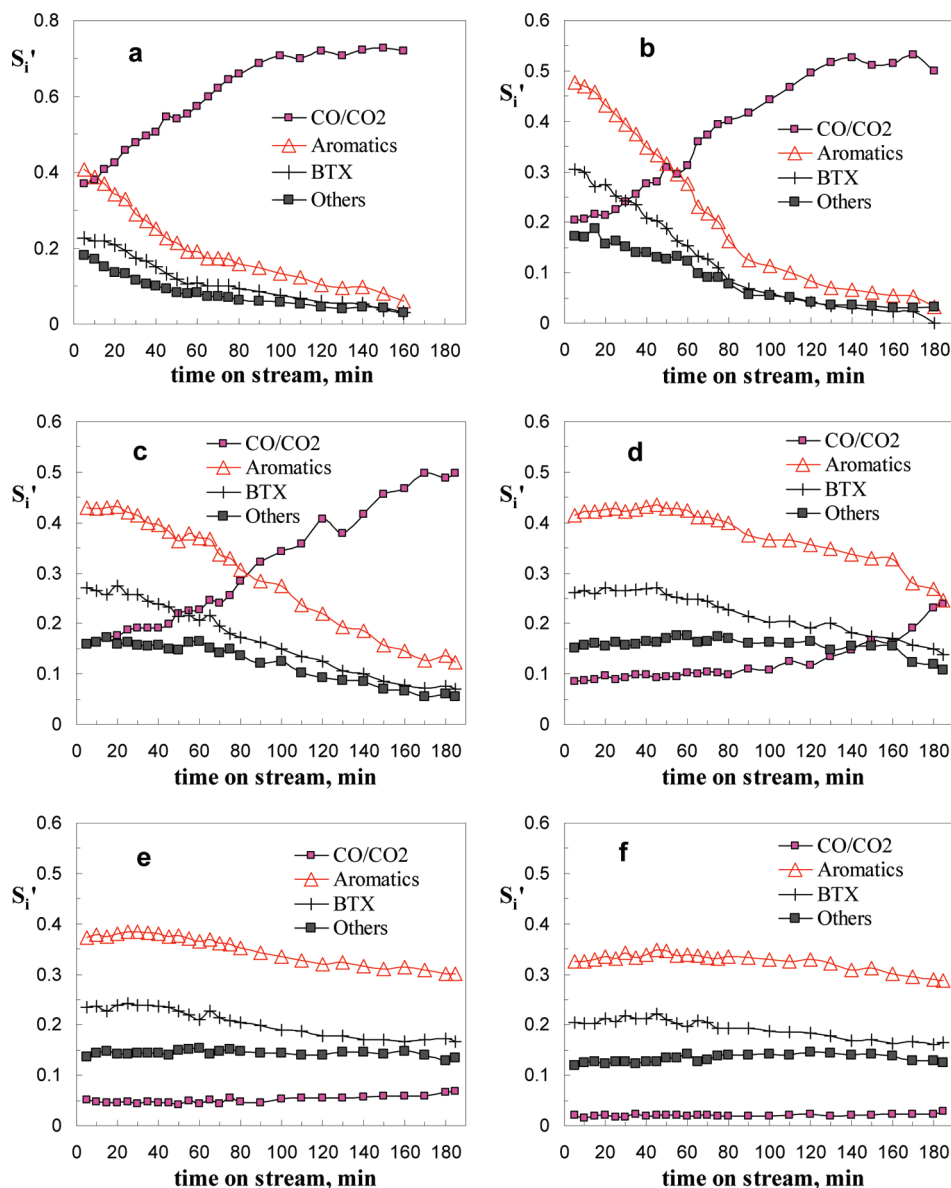


**Figure 6.** Effect of methanol content in the feed on the selectivity of aromatics and of CO + CO<sub>2</sub>: (a) feed, crude bio-oil; (b) feed with 20 wt % methanol; (c) feed with 40 wt % methanol; (d) feed with 60 wt % methanol; (e) feed with 80 wt % methanol; and (f) feed, pure methanol. Reaction conditions: 450 °C;  $W/F_0 = 0.371$  (g of catalyst) h (g of oxygenates)<sup>-1</sup>.

As shown in Figure 5, the methanol content in the feed also has a significant effect on product distribution. The selectivity of aromatics decreases when the methanol content is increased in the feed, whereas the selectivity of light paraffins and nonaromatic C<sub>5+</sub> hydrocarbons increases linearly with the methanol content. The selectivity of light olefins reaches its optimum at a methanol content of ~40 wt %.

Figure 6 shows the effect of the time-on-stream on aromatic selectivity ( $S_i'$ ) calculated by eq 3 but based on the total yield of all products (considering the yield of CO and CO<sub>2</sub>). For a feed of crude bio-oil (Figure 6a), the aromatics selectivity at zero time-on-stream is 0.40, whereas for a feed corresponding to 20 wt % methanol (Figure 6b), it is 0.48. This marked improvement is attributable to the aforementioned effect of CO + CO<sub>2</sub> yield attenuation by co-feeding methanol. For higher contents of methanol in the feed, the selectivity of aromatics decreases slightly when the methanol content is increased. The selectivity of aromatics is 0.32 for the feed of pure methanol (see Figure 6f).

It is important to state that co-feeding methanol attenuates the decrease in the selectivity of aromatics with the time-on-stream. This favorable effect is very pronounced for a methanol content of 60 wt % (see Figure 6d). Under these conditions, the selectivity of aromatics is ~0.40, with a BTX selectivity of 0.25 in the first hour of reaction. The lump named “Other aromatics” corresponds to alkyl monoaromatics (90 wt %) and naphthalene derivatives.

Figure 6 shows that CO + CO<sub>2</sub> selectivity follows a trend that is opposite that of aromatics with the time-on-stream, so that as the time-on-stream is increased, the selectivity of CO + CO<sub>2</sub> increases. Likewise, the effect of co-feeding methanol is a decrease in the selectivity of CO + CO<sub>2</sub>.

Based on the aforementioned results, the co-feeding of 60 wt % methanol is suitable for attaining a high yield and selectivity of BTX, with moderate deactivation and a low yield of CO + CO<sub>2</sub>. This result is due to two factors in the feed: (i) the co-feeding of methanol increases the H/C ratio in the feed, which has a well-known effect in attenuating coke



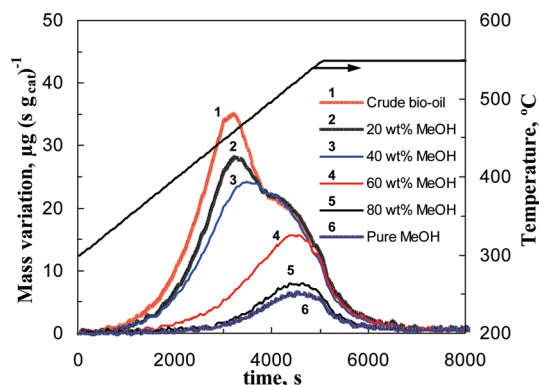


**Figure 7.** Effect of methanol content in the feed on the TPO curves for the combustion of the coke deposited on the catalyst. Reaction conditions: 450 °C;  $W/F_0 = 0.371$  (g of catalyst) h (g of oxygenates)<sup>−1</sup>.

deposition,<sup>24</sup> and (ii) the water content in the feed is 20 wt % (that corresponding to the bio-oil), and this water content is sufficient to have a significant effect in attenuating both the step of oxygenate transformation into hydrocarbons and the deactivation by coke deposition, as is well-known in the literature.<sup>27,38–40</sup>

On the other hand, the results in Figure 6 seem to indicate that, as the capacity of the catalyst for producing hydrocarbons decreases, the production of CO + CO<sub>2</sub> increases, which supports the hypothesis that the hydrocarbon formation reactions compete with those of the decarbonylation and decarboxylation of oxygenates in the bio-oil, and that these latter steps are mainly of thermal origin, with a limited contribution of the catalyst active sites.

The main cause of catalyst deactivation is the deposition of coke on the catalyst. Figure 7 shows the TPO curves obtained in the combustion of the coke deposited on the catalyst after reactions with different methanol contents in the feed. The TPO curve corresponding to a feed of pure MeOH is also shown in this figure. The TPO curves corresponding to crude bio-oil and the bio-oil/methanol mixtures show a heterogeneous coke, in which two peaks can be distinguished. In the combustion of the coke formed when feeding crude bio-oil, the first peak at 450 °C corresponds to a thermal origin coke (pyrolytic lignin, which has not been deposited on the first step of the process). It burns easily because it is deposited outside the catalyst particles and on the particle macropores that comprise the external spaces between HZSM-5 zeolite crystals and bentonite and alumina particles that constitute the matrix of the catalyst. The second peak is not well-defined. It is a shoulder at a temperature above 500 °C and corresponds to the coke of catalytic origin, formed by cyclization–aromatization–condensation reaction mechanisms, which are widely reported in the literature for reactions on microporous acid catalysts.<sup>41,42</sup>

Only one coke of catalytic origin peaking at 510–520 °C is identified in the TPO curve of the coke deposited on the catalyst in the transformation of pure methanol. This temperature is higher than that corresponding to the combustion of the thermal coke, because the catalytic coke is deposited inside the channels of HZSM-5 zeolite crystals and its combustion is limited by internal diffusion and by the

**Table 2.** Effect of Reaction Temperature on the Total Amount of Coke ( $W_{CT}$ ), Total Coke Content in the Catalyst ( $C_{CT}$ ), Mass Fraction of Thermal Coke ( $f_{C1}$ ) and Contents of Thermal Coke ( $C_{C1}$ ) and Catalytic Coke ( $C_{C2}$ )<sup>a</sup>

feed	$C_{CT}$ (wt %)	$f_{C1}$	$C_{C1}$ (wt %)	$C_{C2}$ (wt %)
crude bio-oil	8.11	0.314	2.55	5.56
80 wt % bio-oil/20 wt % MeOH	7.29	0.260	1.89	5.39
60 wt % bio-oil/40 wt % MeOH	6.21	0.181	1.12	5.09
40 wt % bio-oil/60 wt % MeOH	3.48	0.104	0.36	3.11
20 wt % bio-oil/80 wt % MeOH	1.55	0.011	0.02	1.53
MeOH 100%	1.42			1.42
80 wt % bio-oil/20 wt % MeOH (ac)	7.45	0.264	1.97	5.48
60 wt % bio-oil/40 wt % MeOH (ac)	6.98	0.212	1.47	5.51
40 wt % bio-oil/60 wt % MeOH (ac)	5.28	0.196	1.03	4.24
20 wt % bio-oil/80 wt % MeOH (ac)	1.83	0.058	0.11	1.72
MeOH (ac) 100%	1.34			1.34

<sup>a</sup> Reaction conditions: 450 °C;  $W/F_0 = 0.371$  (g of catalyst) h (g of oxygenates)<sup>−1</sup>.

interaction of the acid sites where the coke is partially adsorbed.<sup>30,43</sup>

The thermal coke content ( $C_{C1}$ ) and catalytic coke content ( $C_{C2}$ ) have been quantified by deconvolution of the TPO curves in Figure 7. These results, together with the total coke content ( $C_{CT}$ ) and the thermal coke fraction ( $f_{C1}$ ), are shown in Table 2. The thermal coke fraction decreases considerably as the content of methanol in the feed is increased, and thermal coke is not formed when pure methanol is fed, which confirms the similarity between thermal coke and pyrolytic lignin. The catalytic coke content also decreases as the methanol content in the feed increases, which supports the hypothesis that this coke is more readily formed from bio-oil oxygenate components than from methanol.<sup>22,24</sup>

**3.2. Effect of Temperature in the Catalytic Step.** Figure 8 shows the results of the evolution of product yields at 400 °C (Figure 8a), 450 °C (Figure 8b), and 500 °C (Figure 8c). The feed corresponds to the bio-oil/methanol mixture containing 60 wt % methanol. It is observed that, by increasing the reaction temperature from 400 °C to 450 °C, there is a sharp increase in the yields of hydrocarbons, whereas the increase is less significant when increasing the reaction temperature from 450 °C to 500 °C.

Figure 8 shows that the apparent deactivation (measured by the increase in oxygenate concentration with the time-on-stream and by the lower yields of hydrocarbon products) is significantly lower at 500 °C than at 450 °C. The products that can be considered intermediate in the reaction kinetic scheme, such as C<sub>2</sub>–C<sub>4</sub> olefins and C<sub>5+</sub> hydrocarbons, do not decrease continuously with the time-on-stream, but they peak at 500 °C. Despite catalyst deactivation, the yields of methane and CO+CO<sub>2</sub> increase when temperature is increased and they are almost constant with the time-on-stream, which again confirms that such components are mainly of thermal origin.

The conversion of bio-oil at zero time-on-stream (Figure 9) also increases significantly by increasing the temperature from 400 °C to 450 °C; above this temperature, the increase is small.

There is an important effect of temperature on product distribution (Figure 9). The results show that the dehydrogenation capability of this catalyst (attributable to the nickel content of 1 wt %) increases significantly with temperature and, consequently, the yield of aromatics increases. The yield of nonaromatic C<sub>5+</sub> hydrocarbons decreases with an increase in temperature, which enhances the cracking of these

(40) Gayubo, A. G.; Aguayo, A. T.; Morán, A. L.; Olazar, M.; Bilbao, J. *AIChE J.* **2002**, *48*, 1561–1571.

(41) Guisnet, M.; Magnoux, P. *Appl. Catal., A* **2001**, *212*, 83–96.

(42) Cerqueira, H. S.; Caeiro, G.; Costa, L.; Ramôa Ribeiro, F. *J. Mol. Catal. A: Chem.* **2008**, *292*, 1–13.

(43) Le Minh, C. L.; Jones, R. A.; Craven, I. A.; Brown, T. C. *Energy Fuels* **1997**, *11*, 463–469.



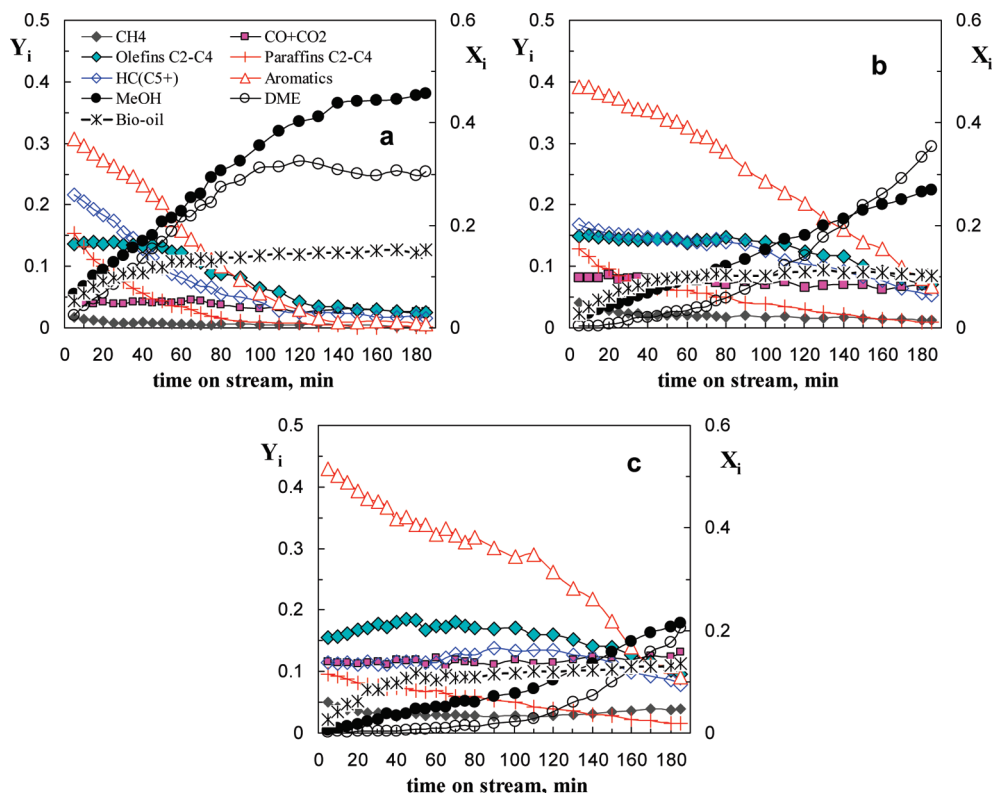


**Figure 8.** Effect of reaction temperature on the evolution with the time-on-stream of product lump yields ( $Y_i$ , left axis) and oxygenate mass fraction ( $X_i$ , right axis) in the reactor outlet stream: (a) 400 °C, (b) 450 °C, and (c) 500 °C. Reaction conditions: feed, bio-oil (40 wt %)/methanol (60 wt %);  $W/F_0 = 0.371$  (g of catalyst) h (g of oxygenates) $^{-1}$ .

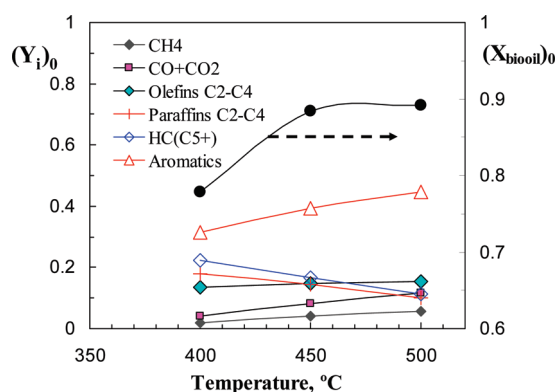


**Figure 9.** Effect of reaction temperature on bio-oil conversion (right axis) and on product lump yields at zero time-on-stream (left axis) in the catalytic transformation step. Reaction conditions: feed, bio-oil (40 wt %)/methanol (60 wt %);  $W/F_0 = 0.371$  (g of catalyst) h (g of oxygenates) $^{-1}$ .

components. The yield of light olefins increases with temperature (as expected, because they are cracking products) but the increase is less than that of aromatic hydrocarbons, and the yield of light paraffins decreases, albeit not as sharply as that of  $C_{5+}$  hydrocarbons. The higher yield of light olefins, compared to light paraffins, is evidence that monomolecular cracking prevails over bimolecular cracking on the HZSM-5 zeolite.<sup>44,45</sup> The yields of methane and CO + CO<sub>2</sub> (mainly thermal cracking products) increase with temperature.

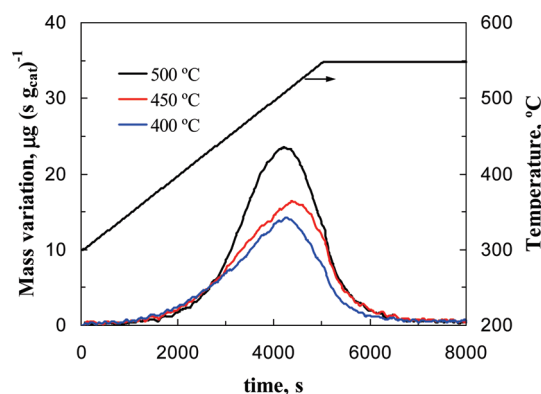


**Figure 10.** Effect of reaction temperature on the TPO curves for the combustion of the coke deposited on the catalyst. Reaction conditions: feed, bio-oil (40 wt %)/methanol (60 wt %);  $W/F_0 = 0.371$  (g of catalyst) h (g of oxygenates) $^{-1}$ .

The above results show that, with the catalyst used, the aromatic hydrocarbons prevail, even at relatively low reaction temperatures (400 °C). In addition, increasing the temperature contributes effectively to increasing the bio-oil conversion (especially in the temperature range of 400–450 °C), as well as the yield and selectivity of aromatics, although there is a significant increase in methane and CO + CO<sub>2</sub> yields at 500 °C.

Figure 10 shows TPO curves for the combustion of the coke deposited on the catalyst at different temperatures. The corresponding values of the total amount of coke ( $W_{CT}$ ), of total coke content, and the amount of each fraction of coke (thermal and catalytic) are listed in Table 3. As observed, the total coke content increases with temperature from

(44) Buchanan, J. S. *Catal. Today* **2000**, 55, 207–212.

(45) Arandes, J. M.; Abajo, I.; Fernández, I.; Azkoiti, M. J.; Bilbao, J. *Ind. Eng. Chem. Res.* **2000**, 39, 1917–1924.

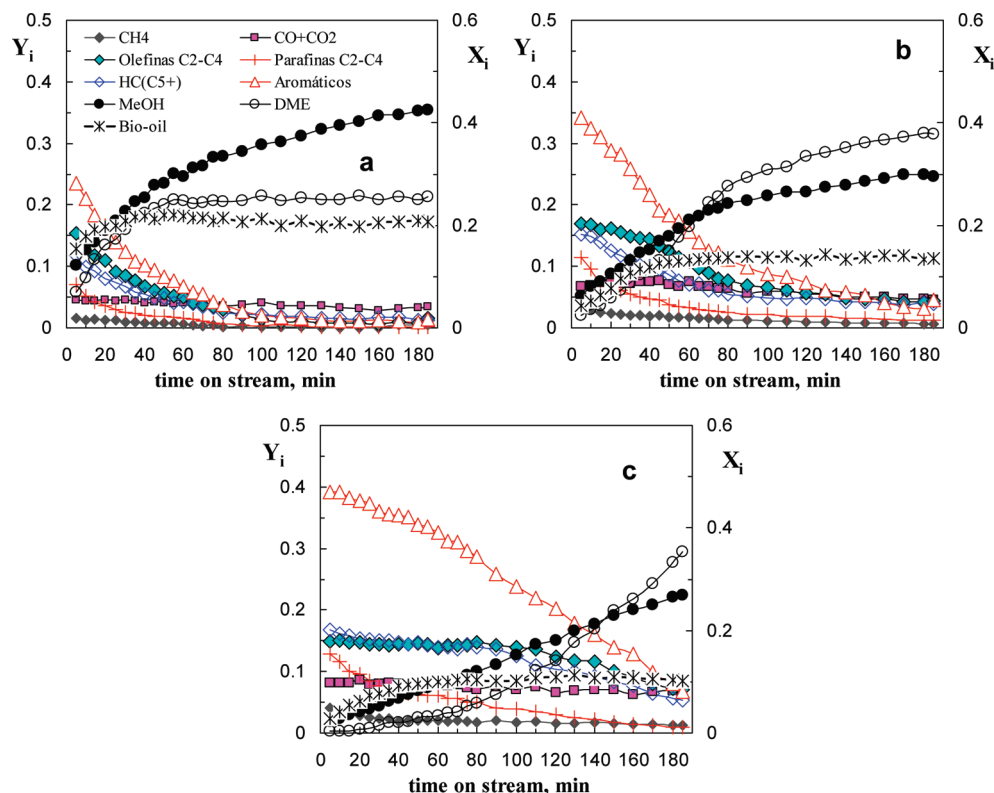


**Figure 11.** Effect of space time on the evolution with the time-on-stream of product lump yields ( $Y_i$ , left axis) and oxygenate mass fraction ( $X_i$ , right axis) in the reactor outlet stream: (a) 0.121 (g of catalyst) h (g of oxygenates) $^{-1}$ , (b) 0.243 (g of catalyst) h (g of oxygenates) $^{-1}$ , and (c) 0.371 (g of catalyst) h (g of oxygenates) $^{-1}$ . Reaction conditions: feed, bio-oil (40 wt %)/methanol (60 wt %); 450 °C.

**Table 3. Effect of Reaction Temperature on the Total Coke Content in the Catalyst ( $C_{CT}$ ), Mass Fraction of Thermal Coke ( $f_{C1}$ ) and Contents of Thermal Coke ( $C_{C1}$ ) and Catalytic Coke ( $C_{C2}$ )<sup>a</sup>**

temperature (°C)	$W_{CT}$ (g)	$C_{CT}$ (wt %)	$f_{C1}$	$C_{C1}$ (wt %)	$C_{C2}$ (wt %)
400	0.073	3.18	0.050	0.16	3.02
450	0.080	3.48	0.104	0.36	3.11
500	0.107	4.67	0.360	1.68	2.99

<sup>a</sup> Reaction conditions: feed, bio-oil (40 wt %)/methanol (60 wt %); mass of catalyst: 2.30 g;  $W/F_0 = 0.371$  (g of catalyst) h (g of oxygenates) $^{-1}$ .

3.18 wt % at 400 °C to 4.67 wt % at 500 °C, because of the increase in thermal coke (pyrolytic lignin) from 0.16 wt % to 1.68 wt %, whereas catalytic coke content is almost constant at a value of ~3 wt %.

The higher deposition of pyrolytic lignin caused by increasing temperature is because temperature enhances the polymerization of lignin pyrolysis phenol-derivatives contained in the bio-oil. The lower catalytic coke deposition is consistent with the aforementioned hypothesis that catalytic coke formation and the resulting deactivation of the catalyst are enhanced by increasing oxygenate concentration in the reaction medium.

**3.3. Effect of Space Time in the Catalytic Step.** Figure 11 shows the results of the evolution with the time-on-stream of product yields and the mass fraction of oxygenates in the feed. The results correspond to a bio-oil/methanol feed with 40 wt % bio-oil and a temperature of 500 °C. Each graph corresponds to a space time value. It is important to state that the apparent deactivation of the catalyst significantly decreases when the space time is increased, which is consistent with the hypothesis that the oxygenates contained in the feed are the main precursors of coke deposition and that the

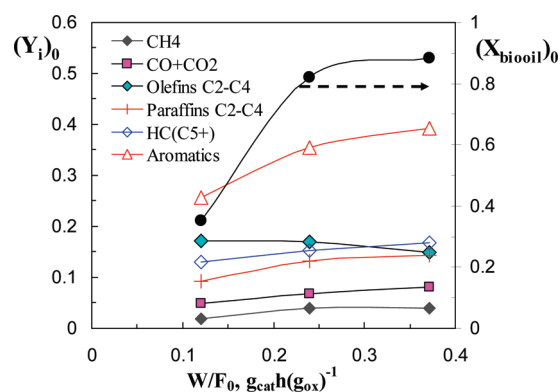


**Figure 12.** Effect of space time on bio-oil conversion (right axis) and on product lump yields at zero time-on-stream (left axis). Reaction conditions: feed, bio-oil (40 wt %)/methanol (60 wt %); 450 °C.

deactivation by coke runs parallel to the reactions of oxygenate transformation into hydrocarbons. This result is coherent with those obtained previously in the transformation of methanol and ethanol to hydrocarbons.<sup>37,46</sup>

Figure 12 shows that there is an increase in hydrocarbon yields at zero time-on-stream, particularly in aromatics, when space time is increased. Methane and CO + CO<sub>2</sub> yields increase slightly with space time, which is evidence of a partial catalytic origin of CO and CO<sub>2</sub> apart from the aforementioned thermal origin, which can be attributed to the decarbonylation and decarboxylation capability of nickel catalysts. The maximum yield of olefins observed for the lowest value of space time studied is due to the primary

(46) Aguayo, A. T.; Gayubo, A. G.; Atutxa, A.; Olazar, M.; J. Bilbao, J. *Ind. Eng. Chem. Res.* **2002**, *41*, 4216–4224.

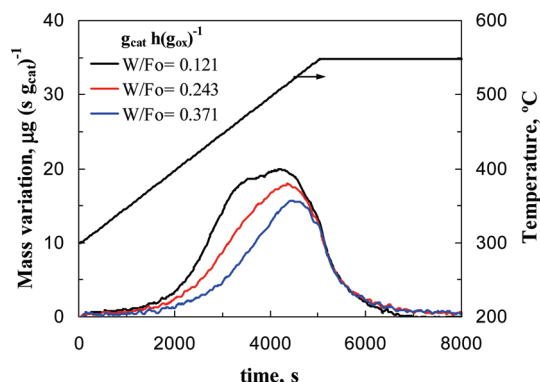


**Figure 13.** Effect of space time on the TPO curves for the combustion of the coke deposited on the catalyst. Reaction conditions: feed, bio-oil (40 wt %)/methanol (60 wt %); 450  $^{\circ}\text{C}$ .

**Table 4.** Effect of Space Time on the Total Yield of Coke ( $Y_{\text{CT}}$ ), Total Coke Content in the Catalyst ( $C_{\text{CT}}$ ), Mass Fraction of Thermal Coke ( $f_{\text{CT}}$ ) and the Contents of Thermal Coke ( $C_{\text{CT}}$ ) and Catalytic Coke ( $C_{\text{C2}}$ )<sup>a</sup>

$W/F_o$ ( $\text{g}_{\text{cat}}\text{h (g}_{\text{ox}})^{-1}$ )	$Y_{\text{CT}}$ ( $(\text{g}_{\text{coke}})(\text{g}_{\text{feed}})^{-1}$ )	$C_{\text{CT}}$ (wt %)	$f_{\text{CT}}$	$C_{\text{CT}}$ (wt %)	$C_{\text{C2}}$ (wt %)
0.121	$1.55 \times 10^{-3}$	5.08	0.183	0.93	4.15
0.243	$2.55 \times 10^{-3}$	4.17	0.121	0.50	3.90
0.371	$3.30 \times 10^{-3}$	3.48	0.104	0.36	3.11

<sup>a</sup> Reaction conditions: feed, bio-oil (40 wt %)/methanol (60 wt %); 450  $^{\circ}\text{C}$ .

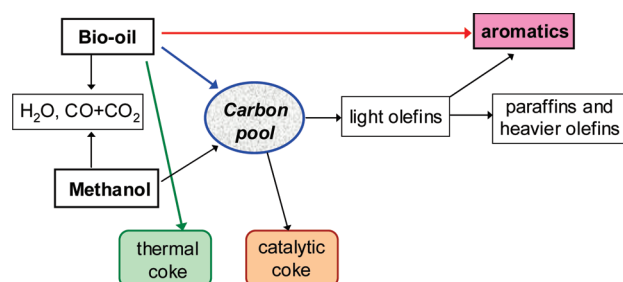
product nature of these olefins in the transformation of methanol and bio-oil oxygenates.

Figure 12 also shows the effect of space time on the conversion at zero time-on-stream of the bio-oil fed in the bio-oil/methanol mixture. Note that a space time of  $>0.3$  (g of catalyst) h (g of oxygenates)<sup>−1</sup> is required to reach a conversion of  $\sim 90$  wt %.

Figure 13 shows the TPO combustion curves of the coke deposited on the catalyst during the experiments with different values of space time. The values of thermal and catalytic coke fractions, listed in Table 4, together with the results for total coke content and total yield of coke ( $Y_{\text{CT}}$ ), have been determined by deconvolution of the TPO curves.

The results in Table 4 show that the total yield of coke (mainly of catalytic origin) increases with space time, whereas the total coke content in the catalyst decreases with space time, because of the decrease in thermal and catalytic coke contents. The overall yield of thermal coke is practically constant, and by increasing space time, the same amount is distributed on a larger amount of catalyst, leading to the aforementioned lower relative content. The overall yield of catalytic coke increases with space time from  $1.27 \times 10^{-3}$  (g of coke) (g of oxygenates)<sup>−1</sup> for 0.121 (g of catalyst) h (g of oxygenates)<sup>−1</sup> up to  $2.96 \times 10^{-3}$  (g of coke) (g of oxygenates)<sup>−1</sup> for 0.371 (g of catalyst) h (g of oxygenates)<sup>−1</sup>, because of the involvement of acid sites in coke formation.

**3.4. Simplified Kinetic Scheme.** Based on the results of previous sections, the simplified kinetic scheme in Figure 14 is proposed, which shows the steps for hydrocarbon formation from the bio-oil/methanol mixture. This scheme considers the participation of bio-oil oxygenates as reactants in the “carbon pool” mechanism, which is well-established in



**Figure 14.** Kinetic scheme for the transformation of the bio-oil/methanol mixtures into hydrocarbons in the 400–500  $^{\circ}\text{C}$  range on Ni-HZSM-5 zeolite.

the literature for explaining the formation of light olefins as primary products in the transformation of methanol.<sup>39,47–49</sup>

According to the scheme presented in Figure 14, aromatics are formed from bio-oil via two routes: (i) via direct deoxygenation (dehydration, decarboxylation, decarbonylation)—cracking of high-molecular-weight oxygenates; (ii) by means of the participation of bio-oil oxygenates in the carbon pool mechanism. These oxygenates will be transformed into alkylarenes, which are intermediate compounds in olefin formation that, at the same time, condense to form the polyaromatics that comprise the coke of catalytic origin.

In this scheme, the coke of thermal origin will correspond to that denoted pyrolytic lignin, which is formed mainly by the polymerization of the lignin pyrolysis derived compounds that have reached the catalytic bed, because they have not polymerized in the previous thermal step built for that purpose.

The deactivation of the catalyst by coke deposition on the acid sites will cause the decrease in the reaction rates of the catalytic steps, whereas the thermal origin steps will be favored by the higher concentration of oxygenates in the reaction medium. This explains the fact that the yield of CO + CO<sub>2</sub> remains almost constant as the catalyst is being deactivated.

## Conclusions

The transformation of crude bio-oil in an online two-step (thermal-catalytic) process is postulated as a solution to the problems inherent to the catalytic transformation of crude bio-oil. In the catalytic transformation step, a conversion of bio-oil of  $>90$  wt % is achieved using a HZSM-5 zeolite catalyst with 1 wt % nickel at 450  $^{\circ}\text{C}$  and with moderate space time (0.371 (g of catalyst) h (g of oxygenates)<sup>−1</sup>), and an aromatics selectivity of 0.65 (excluding CO and CO<sub>2</sub> formed). Nevertheless, there is an important drawback in the treatment of crude bio-oil, namely, the rapid catalyst deactivation caused by the deposition of coke of thermal and catalytic origin.

The results seem to indicate that the reactions of hydrocarbon formation compete with those of decarbonylation and decarboxylation, and methanol co-feeding helps to improve this competence by mitigating the yield of CO and CO<sub>2</sub>. Consequently, as the catalyst is being deactivated, the reactions of hydrocarbon formation (catalyzed by the acid sites) are mainly affected and the steps of decarbonylation and decarboxylation of bio-oil components are enhanced.

(48) Gayubo, A. G.; Vivanco, R.; Alonso, A.; Valle, B.; Aguayo, A. T. *Ind. Eng. Chem. Res.* **2005**, *44*, 6605–6614.

(49) Aguayo, A. T.; Gayubo, A. G.; Vivanco, R.; Alonso, A.; Bilbao, J. *Ind. Eng. Chem. Res.* **2005**, *44*, 7279–7286.

(47) Haw, J. F.; Nicholas, J. B.; Song, W.; Deng, F.; Wang, Z.; Xu, T.; Heneghan, C. S. *J. Am. Chem. Soc.* **2000**, *122*, 4763–4775.

The co-feeding of methanol with crude bio-oil has a significant effect of reducing coke deposition, which is the main cause of catalyst deactivation. This effect, which increases with methanol content in the feed, is attributable to two factors: (i) coke formation from methanol is lower than that from oxygenate components in the bio-oil; and (ii) the water generation in the dehydration of methanol on the catalyst acid sites contributes to inhibiting coke formation. Nevertheless, a very high content of methanol in the feed also has an unfavorable effect on the conversion of the bio-oil contained in the bio-oil/methanol mixture, because the presence of water also decreases the rate of the catalytic transformation steps of bio-oil oxygenate components. A feed of 40 wt % bio-oil/60 wt % methanol is suitable for balancing these two effects. Under these conditions, the selectivity of aromatics is  $\sim 0.40$ , with a BTX selectivity of 0.25 in the first reaction hour. The remaining aromatics are alkyl monoaromatics (90 wt %) and naphthalene derivatives.

The conversion of the bio-oil contained in the mixture (methanol conversion at zero time-on-stream is complete under the conditions studied) increases with temperature in the 400–500 °C range, but at the expense of increasing the yields of methane and CO + CO<sub>2</sub>. Aromatic hydrocarbons prevail and the selectivity of C<sub>2</sub>–C<sub>4</sub> olefins increases with temperature, in parallel with a decrease in C<sub>5+</sub> hydrocarbons.

By increasing the space time in the range of 0.121–0.371 (g of catalyst) h (g of oxygenates)<sup>−1</sup>, the yield of aromatics significantly increases and the yields of C<sub>5+</sub> hydrocarbons, C<sub>2</sub>–C<sub>4</sub> paraffins, methane, and CO + CO<sub>2</sub> increase, to a lesser extent, whereas the yield of C<sub>2</sub>–C<sub>4</sub> olefins decreases.

The results of the temperature-programmed oxidation (TPO) curves of coke combustion show that an increase in temperature and space time helps to decrease coke content in the catalyst, which contributes to maintaining its activity. This result may be a consequence of the fact that coke precursors

are mainly oxygenate compounds, whose concentration in the reaction medium decreases as temperature and space time are increased.

**Acknowledgment.** This work was performed with the financial support of the Department of Education, Universities and Research of the Basque Government (Project GIC07/24-IT-220-07) and of the Ministry of Science and Innovation of the Spanish Government (Project CTQ2006-12006/PPQ).

### Notation

- $C_{ci}$  = content of coke fraction  $i$  in the catalyst ( $i = 1$ , thermal coke;  $i = 2$ , catalytic coke)
- $d_p$  = pore diameter (Å)
- $F_0$  = mass flow of oxygenates (in bio-oil and methanol) fed into the reactor (g h<sup>−1</sup>)
- $f_{c1}$  = mass fraction of thermal origin coke in the catalyst
- $(m_{\text{bio-oil}})_i$  = mass flow of bio-oil at the reactor inlet (g h<sup>−1</sup>)
- $(m_{\text{bio-oil}})_o$  = mass flow of bio-oil at the reactor outlet (g h<sup>−1</sup>)
- $S_i$  = selectivity of product lump  $i$ , expressed by mass unit of total product amount excluding CO and CO<sub>2</sub>
- $S'_i$  = selectivity of product lump  $i$ , expressed by mass unit of total product amount
- $S_{\text{BET}}$  = BET specific surface (m<sup>2</sup> g<sup>−1</sup>)
- $T$  = temperature (°C)
- $t$  = time-on-stream (h)
- $V_p$  = pore volume (cm<sup>3</sup> g<sup>−1</sup>)
- $W$  = mass of catalyst (g)
- $W_{\text{CT}}$  = total amount of coke (g)
- $X_i$  = lump  $i$  concentration, given as a mass fraction on a water-free basis
- $X_{\text{bio-oil}}$  = bio-oil conversion
- $Y_i$  = yield of product lump  $i$
- $Y_{\text{CT}}$  = total yield of coke ((g of coke)/(g of oxygenates in the feed)<sup>−1</sup>)